CrystEngComm

RSC Publishing

PAPER

View Article Online
View Journal | View Issue

Cite this: *CrystEngComm*, 2013, **15**, 9729

Copper(II) coordination polymers of $imdc^-$ (H_2imdc^+ = the 1,3-bis(carboxymethyl)imidazolium cation): unusual sheet interpenetration and an unexpected single crystal-to-single crystal transformation†

Brendan F. Abrahams,*[a] Helen E. Maynard-Casely,[b] Richard Robson*[a] and Keith F. White[a]

Received 25th June 2013,
Accepted 29th August 2013

DOI: 10.1039/c3ce41226a

www.rsc.org/crystengcomm

The monoanion of 1,3-bis(carboxymethyl)imidazolium (H_2imdc^+) combines with Cu(II) to produce an undulating 2D coordination polymer of composition $[Cu_2(imdc)_2(CH_3OH)_2](BF_4)_2{\cdot}(CH_3OH)(H_2O)$ (**1**) in which copper acetate-like dimers, linked by $imdc^-$ ligands, act as 4-connecting centres. Cationic sheets stack on top of each other in an A, B, A, B… fashion and produce a structure that contains channels running parallel to the plane of network. Tetrafluoroborate anions are located in channels between sheets. Upon removal of coordinated and non-coordinated solvent molecules a single crystal-to-single crystal transformation occurs to yield a similar compound but with BF_4^- anions now coordinated. CO_2 isotherms measured at 258 and 273 K show only modest uptake of CO_2 but provide an indication that the sheets move apart at elevated pressures in order to accommodate the guest molecules. A compound of composition $[Cu_3(OH)_2(imdc)_2]{\cdot}SiF_6{\cdot}2H_2O{\cdot}2MeOH$ (**3**), which possesses a 3D network, is formed by the combination of copper(II) acetate, copper(II) hexafluorosilicate and Himdc. In this structure infinite parallel $Cu_3(OH)_2$ chains are linked by bridging $imdc^-$ ligands to form channels that have an approximately triangular cross-section. These channels are occupied by SiF_6^{2-} anions in addition to solvent molecules. When copper(II) acetate is combined with Himdc in the appropriate ratio, a 1D coordination polymer of composition $Cu(imdc)_2$ (**4**) is formed in which pairs of $imdc^-$ anions bridge Cu(II) centres. When the reaction is performed in the presence of $NaBF_4$ a minor crystalline product with tetragonal symmetry is isolated in addition to the 1D coordination polymer. This compound of composition $Cu_2(imdc)_4NaBF_4{\cdot}7H_2O$ (**5**) consists of 2D $Cu(imdc)_2$ networks and features an unusual mode of interpenetration.

Introduction

As part of a general exploration of lightweight framework materials containing anionic binding groups with a cationic core, we became interested in the "zwitterionic" monoanion of 1,3-bis(carboxymethyl)imidazolium (H_2imdc^+). We were interested in investigating whether such a ligand, within a network structure, is able to provide a flat, positively charged surface that may lead to enhanced physisorption compared to a ligand with an uncharged aromatic core. Prior to the work reported here, we were initially interested in the combination of this potentially bridging ligand with metal ions such as Li^+ and Mg^{2+}, however a survey of the literature revealed that whilst a number of metal-imdc complexes involving s-,[1] p-,[2] d-[3] and f-block[4] metal cations have been structurally characterised, no Cu(II) complexes have been investigated. Although coordination polymers generated by the combination of Cu(II) with bis(carboxylate) ligands are well known, we were interested in exploring whether the use of a dicarboxylate ligand that possessed only a single negative charge would lead to coordination networks with unusual structural features.

In this current work we describe five different coordination polymers formed from the combination of H_2imdc^+ or Himdc and Cu(II) under various conditions.

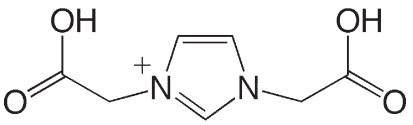

$[H_2imdc]^+$

[a] *School of Chemistry, University of Melbourne, Victoria 3010, Australia. E-mail: bfa@unimelb.edu.au, r.robson@unimelb.edu.au; Fax: +61 3 9347 5180*
[b] *Australian Synchrotron, 800 Blackburn ClaytonVictoria 3168, Australia*

† Electronic supplementary information (ESI) available: Supplementary figures including powder diffraction patterns, infrared spectra and thermogravimetric data. CCDC 907228, 946321–946324. For ESI and crystallographic data in CIF or other electronic format see DOI: 10.1039/c3ce41226a

Results and discussion

$[Cu_2(imdc)_2(CH_3OH)_2](BF_4)_2{\cdot}(CH_3OH)(H_2O)$ and $[Cu_2(imdc)_2(BF_4)_2]$

The combination of a methanolic solution of $[H_2imdc]Cl$ and an aqueous solution of $Cu(BF_4)_2$in a 1 : 1.25 ratio yields orthorhombic crystals of composition, $[Cu_2(imdc)_2(CH_3OH)_2](BF_4)_2{\cdot}(CH_3OH)(H_2O)$ (**1**). Within this structure, copper acetate-type dimeric units are linked by four $imdc^-$ ligands to four other symmetry related binuclear Cu(II) units (Fig. 1a) within an undulating 2D network that has the topology of a 4,4 net (4-connected nodes with the shortest circuit between pairs of connections being 4-membered circuits). The two axial positions on each binuclear unit are occupied by methanol molecules. The separation between the midpoints of pairs of binuclear units, bridged by the $imdc^-$ ligands, is 10.69 Å. When the network is viewed in projection along a direction normal to the plane of the polymer, rhombic almost square frames are apparent. The separation of binuclear units occupying opposite corners of each frame correspond to the *b* and *c* cell lengths *i.e.* 12.7971(3) and 14.4678(3) Å respectively. In the extended structure, layers of the 2-D network stack along the *a* axis in an A, B, A, B… fashion (Fig. 1b). When the packing of the 2-D sheets is viewed edge-on down the *b*-axis (Fig. 1c), it can be seen that the $[Cu_2(imdc)_2(CH_3OH)_2]^{2+}$ layers are out of phase with each other leading to channels that run parallel to the *b* direction. Disordered solvent molecules are located within the channels. BF_4^- anions are clearly apparent within the channels although they do exhibit significant orientational disorder (see ESI† for further details).

The presence of solvent-filled channels in the crystal provided encouragement that the compound may serve as a host for molecules such as carbon dioxide upon desolvation. Thermogravimetric analysis (Fig. S1a†) reveals that the compound loses solvent under ambient conditions and the solvent loss continues as the temperature is raised. At a temperature of 215 °C thermal degradation of the compound occurs, however when crystals of $[Cu_2(imdc)_2(CH_3OH)_2](BF_4)_2{\cdot}(CH_3OH)(H_2O)$ are dried at a temperature of 135 °C in an oven they are found to undergo an unexpected single crystal-to-single crystal transformation to yield the desolvated framework, $[Cu_2(imdc)_2(BF_4)_2]$ (**2**); thus the thermal degradation that occurs at 215 °C corresponds to the decomposition of the desolvated compound, **2**. A single crystal structure determination of the solvent-free solid indicates the presence of undulating 2D networks similar to that described above. Of particular interest in the transformed crystal are the BF_4^- anions which are now located in the two axial positions of each binuclear unit, sites that were occupied by coordinated methanol in the parent crystal (Fig. 2a). Although there is a small degree of disorder associated with the orientation of the coordinated BF_4^- anions (see ESI† for further details), the tetrahedral anions are more clearly defined than when they were surrounded by solvent molecules within the channels. With the anions now serving as appendages to the $[Cu_2(imdc)_2]^{2+}$

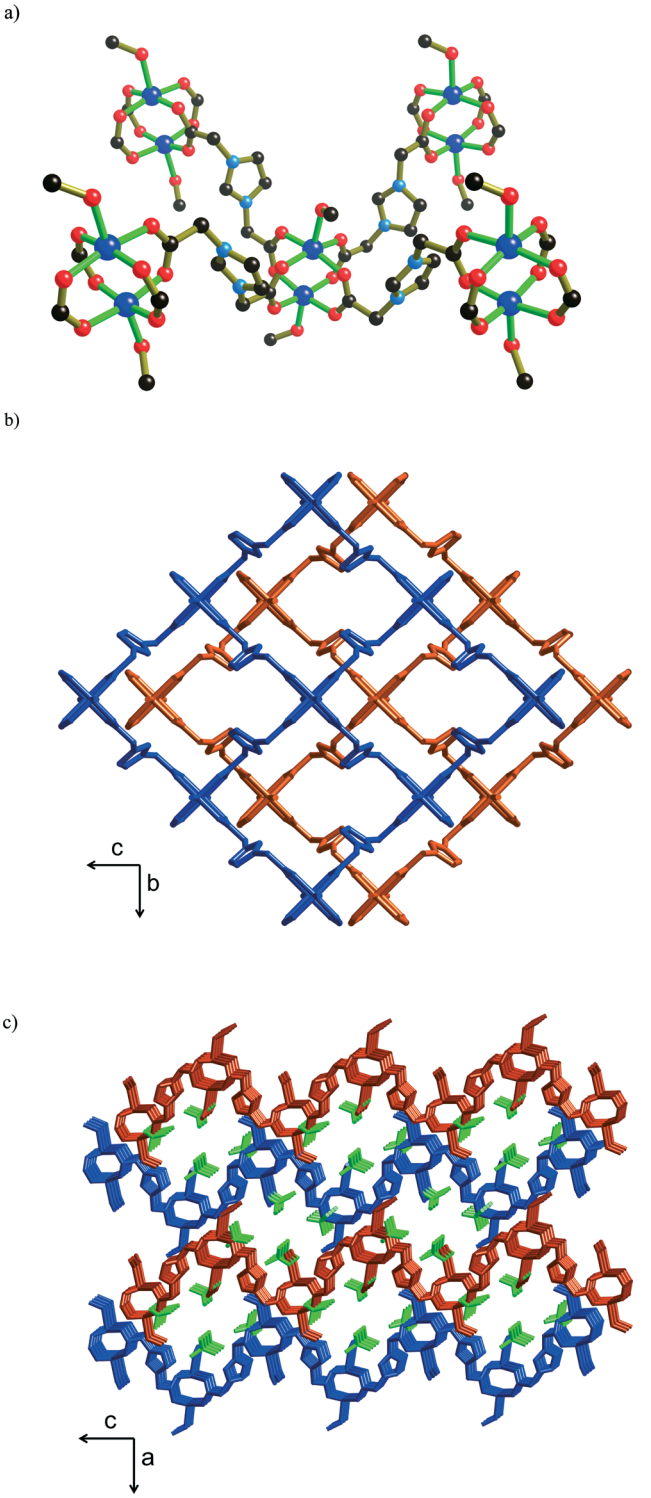

Fig. 1 The structure of $[Cu_2(imdc)_2(CH_3OH)_2](BF_4)_2{\cdot}$solvate (**1**) showing: a) part of the undulating $[Cu_2(imdc)_2(CH_3OH)_2]^{2+}$ square grid sheet in which Cu_2 units are bridged by $imdc^-$ anions; coordinate bonds are indicated by green connections, atom colour code: Cu – deep blue, O – red, N – light blue, C – black b) a stick representation indicating the relative arrangement of the 2D networks viewed along the stacking direction (along the *a* axis); the methyl groups of the methanol have been omitted for clarity c) a view almost normal to the stacking direction showing the channels between the sheets that run parallel to the *b* axis; the BF_4^- anions are indicated in green. Non-coordinated solvent molecules and hydrogen atoms have been omitted for clarity.

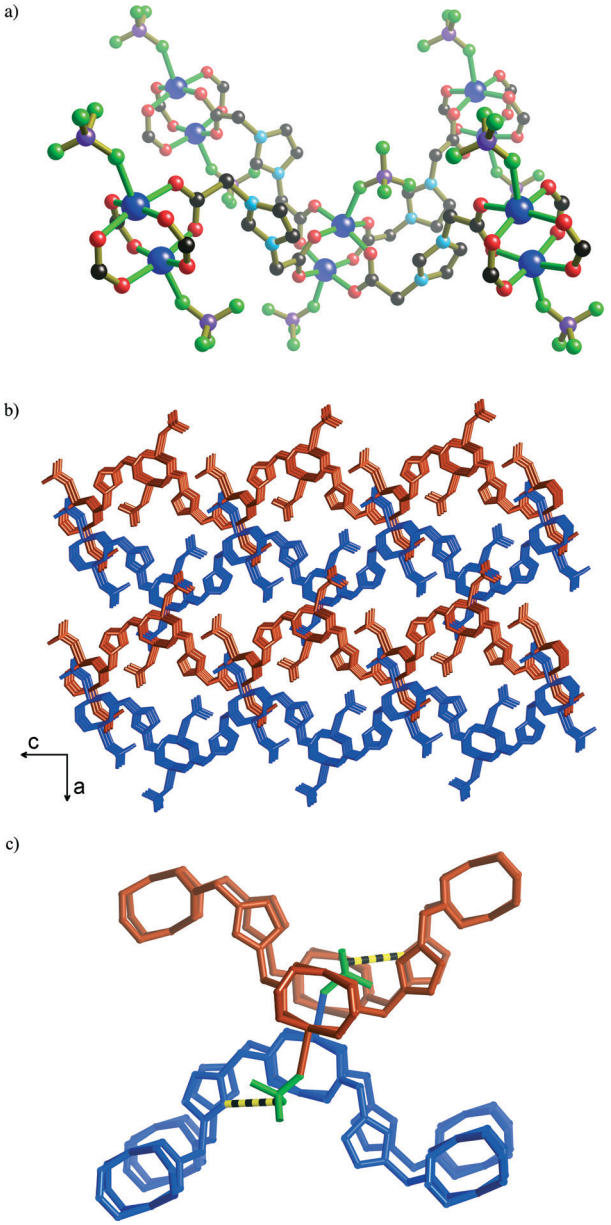

Fig. 2 The structure of $[Cu_2(imdc)_2(BF_4)_2]$ (**2**) showing: a) part of the undulating $[Cu_2(imdc)_2(BF_4)_2]$ square grid sheet in which Cu_2 units are bridged by $imdc^-$ anions; coordinate bonds are indicated by green connections, atom colour code: Cu – deep blue, F – green, O – red, N – light blue, C – black, B – purple b) a stick representation indicating the relative arrangement of the 2D networks viewed almost normal to the stacking direction (along the *a* axis); c) the C–H···F hydrogen bonding interaction, indicated by yellow and black striped connections, between sheets involving the coordinated BF_4 anion and an imidazolium proton; BF_4 anions are represented by green connections. Hydrogen atoms have been removed for clarity.

polymer the desolvation process results in the transformation of the 2D cationic network into a neutral network.

The space group remains the same following the desolvation process and not surprisingly the cell is smaller in the desolvated crystal, with the cell volume shrinking from 3078.29(11) to 2686.1(6) $Å^3$, a decrease of 12.7%. Of particular interest are the changes to the unit cell lengths. The *a* cell length which corresponds to the stacking direction of the sheets decreases from 16.6263(3) to 15.6203(16) Å indicating that upon solvent loss the 2D networks move closer together. A significant compression along the *b* axis from 12.7971(3) to 11.564(2) Å is apparent which is accompanied by an expansion from 14.4678(3) to 14.8705(14) Å along the *c* direction. Thus the rhombic appearance of the frames is accentuated in the desolvated structure (ESI,† Fig. S1e). In addition to the changes in separations across the frames, the separation between the centres of the binuclear nodes has decreased from 10.69 to 10.39 Å.

Another subtle but nevertheless significant difference relates to the relative positions of adjacent sheets. In the description of the solvated structure represented above, the comment was made that the sheets are "out of phase" when viewed down the *b* axis. In the desolvated structure the sheets are even closer to being fully out-of-phase when viewed down the *b* axis (Fig. 2b). A possible explanation for the alignment of the layers is the presence C–H···F hydrogen bonding interactions (3.10 Å) between a coordinated BF_4^- anion on one network and an imidazolium proton (bound to the carbon atom in the 2-position of the imidazole ring) on an adjacent network, indicated by back and yellow striped connections in Fig. 2c. Intrasheet C–H···F hydrogen bonds involving the second type of coordinated BF_4^- anion and methylene protons are also present (3.04 Å). When viewed along the *c* axis the sheets are "in phase" in both the solvated (**1**) and de-solvated (**2**) forms although changes are apparent in shape of the sheet (ESI,† Fig. S1f). Although the structure of the desolvated crystal provided data that allowed an accurate structure determination, the diffraction peaks were found to be significantly broader following desolvation. The decrease in quality of the diffraction is indicated by a relatively high R_{int} value for the desolvated form (0.1062) compared to the solvated form (0.0186).

Following the suggestion of a referee, the transformation of a single crystal upon desolvation was followed using single crystal X-ray diffraction. As expected a structure determination on a full set of data collected on a crystal at 130 K indicated an essentially identical structure to that described above for **1**. Upon completion of the data collection the crystal was warmed in a stream of nitrogen to a temperature of 400 K. During this warming process visual inspection of the crystal revealed some deterioration of the crystal accompanying the loss of solvent. After being held at 400 K for 20 minutes the crystal was cooled back to 130 K. The diffraction peaks had now become quite broad and indicated significant fragmentation of the crystal. Despite the fragmentation it was possible to measure a data set associated with one of the daughter fragments. This data set confirmed that the BF_4^- anions were now coordinated to the Cu(II) centres.

The presence of channels in the cationic framework prompted an investigation of the ability of the compound to sorb carbon dioxide. A bulk sample of $[Cu_2(imdc)_2(CH_3OH)_2](BF_4)_2{\cdot}(CH_3OH)(H_2O)$ was heated to 120 °C under dynamic vacuum to remove the solvent molecules from the crystal. CO_2 sorption isotherms were measured at 258 and 273 K.

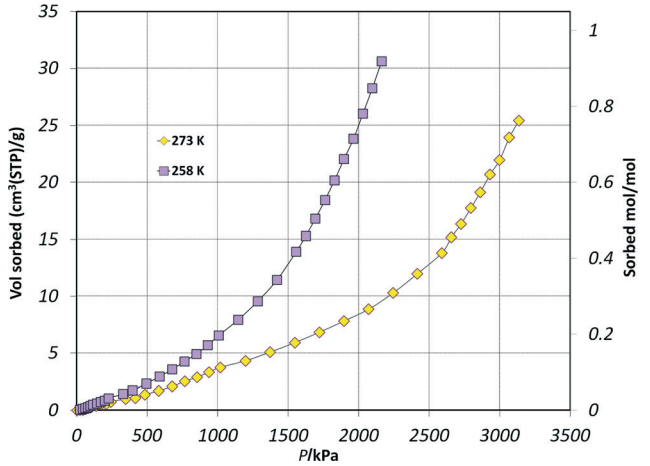

Fig. 3 CO_2 sorption isotherms of $[Cu_2(imdc)_2(BF_4)_2]$ (**2**) measured at 258 (purple squares) and 273 K (yellow diamonds) in [Vol CO_2 cm^3(STP) per g)] and [mol (CO_2) per mol $[Cu_2(imdc)_2](BF_4)_2$.

Fig. 3 indicates only modest uptake of CO_2, however the isotherm shape signals unusual sorption behaviour. The isotherms reveal that at pressures below 1 atm, very little CO_2 is sorbed by the compound but as the pressure of CO_2 is increased further, significant quantities of CO_2 are sorbed. These isotherms follow a type III isotherm path.[5]

The heat of CO_2 sorption (ΔH_{sorp}) was calculated by fitting data from the 258 and 273 K isotherms to a virial-type equation. The sorption enthalpy over the CO_2 loading range is presented in ESI,† Fig. S1g. At initial CO_2 loading the ΔH_{sorp} is −19.6 kJ mol^{-1}. However, the graph indicates that as more CO_2 binds to the surfaces of the framework the compound exhibits a greater affinity for CO_2. This is shown by an upturn in the graph, which indicates at the highest measured loading (1.4 mmol of CO_2 per g) ΔH_{sorp} has increased to −22.9 kJ mol^{-1}.

The type III sorption behaviour is indicative of cooperativity in the binding of CO_2 and is consistent with structural changes occurring in the material upon sorption of CO_2; unusual sorption behaviour in the past has been attributed to structural changes within the sorbent material during gas sorption.[6] The remarkable structural changes that occur upon desolvation (described above) indicate that the layers are able to move relative to each other with retention of crystallinity. We propose that as the pressure of the gas is increased, the layers are forced further apart facilitating the uptake of larger quantities of carbon dioxide and access to surfaces that have a higher affinity for carbon dioxide.

$[Cu_3(OH)_2(imdc)_2]\cdot SiF_6\cdot 2H_2O\cdot 2MeOH$

The structures described above provided encouragement that it may be possible to obtain a similar type of $[Cu_2(imdc)_2]^{2+}$ network with anions other than BF_4^-. The prospect of using the potentially bridging, SiF_6^{2-} anion as a counterion for the $[Cu_2(imdc)_2]^{2+}$ network was attractive because it opened up the possibility of linking the 2D $[Cu_2(imdc)_2]^{2+}$ sheets into a 3D network. Whilst our attempts to generate such a compound were unsuccessful an unusual coordination polymer of composition, $[Cu_3(OH)_2(imdc)_2]SiF_6\cdot 2H_2O\cdot 2MeOH$ (**3**), was obtained by the combination of $Cu(OAc)_2$, Himdc and $CuSiF_6$ in an aqueous methanolic solution.

The structure determination indicates a 3D network composed of infinite parallel chains formed from Cu(II) centres linked by hydroxide and carboxylate groups (Fig. 4a). Within the chains there are three crystallographically unique Cu(II) centres, two of which have a square pyramidal coordination environment whilst the third has an octahedral environment. There are two types hydroxide ion, each of which binds to the three crystallographically distinct Cu(II) centres. The hydroxide bridges lead to the formation of a continuous chain that is indicated by green connections in Fig. 4a. Carboxylate groups from $imdc^-$ ligands surround the chain and complete the coordination environments of the Cu(II) centres. The carboxylate groups belong to $imdc^-$ ligands that act as bridges between pairs of identical Cu(II)-hydroxide chains. The ligands extend outwards to six equivalent Cu(II)-hydroxide chains leading to the formation of an infinite 3D network possessing channels with an approximately trigonal cross-section that run parallel to the direction of the Cu(II)-hydroxide chains (Fig. 4b). Channel "walls", which are formed from bridging $imdc^-$ ligands, are of two types; the first type which lies parallel with the *a*–*c* plane contains symmetry related bridging ligands with two distinct orientations as indicated in Fig. 4c. Each carboxylate group of these ligands coordinates in a μ_3 fashion. The ligands in the channel wall are separated from adjacent ligands by distances corresponding to half the length of the *c* cell dimension. The mean plane of the second type of channel wall is inclined to the *a*–*c* plane and consists of bridging ligands separated by an interval equal to the length of the *c* cell dimension *i.e.* half the frequency of that found in the first type of channel wall as indicated in Fig. 4d. The carboxylate groups of these $imdc^-$ ligands coordinate in a μ_2 manner.

The channels within the structure are filled with methanol and water molecules in addition to SiF_6^{2-} anions. The solvent molecules form hydrogen bonds with the cationic $[Cu_3(OH)_2(imdc)_2]^{2+}$ framework and SiF_6^{2-} anions. There are also C–H···F hydrogen bonds of 2.99 and 3.00 Å involving aromatic protons and fluorine atoms of the SiF_6^{2-} anions.

$Cu(imdc)_2$ and $Cu_2(imdc)_4NaBF_4\cdot 7H_2O$

The reaction that led to the generation of the aforementioned compound of formula $[Cu_2(imdc)_2(CH_3OH)_2](BF_4)_2\cdot(CH_3OH)(H_2O)$ (**1**) involved the combination of Cu(II), BF_4^- and H_2imdc^+ in a 1.25 : 2.5 : 1 ratio. With a view to generating this sample by combining the components in the stoichiometric ratio found in the product, $Cu(OAc)_2$, $NaBF_4$ and Himdc were combined in an aqueous methanol solution in a 1 : 1 : 1 ratio. The reaction initially results in the separation of a mixture of two visibly different types of crystals. The first type, which forms as chunky blue crystals, many with octahedral morphology, has the composition $Cu_2imdc_4NaBF_4\cdot 7H_2O$. The second form consists of blue plate-like crystals of composition $Cu(imdc)_2$.

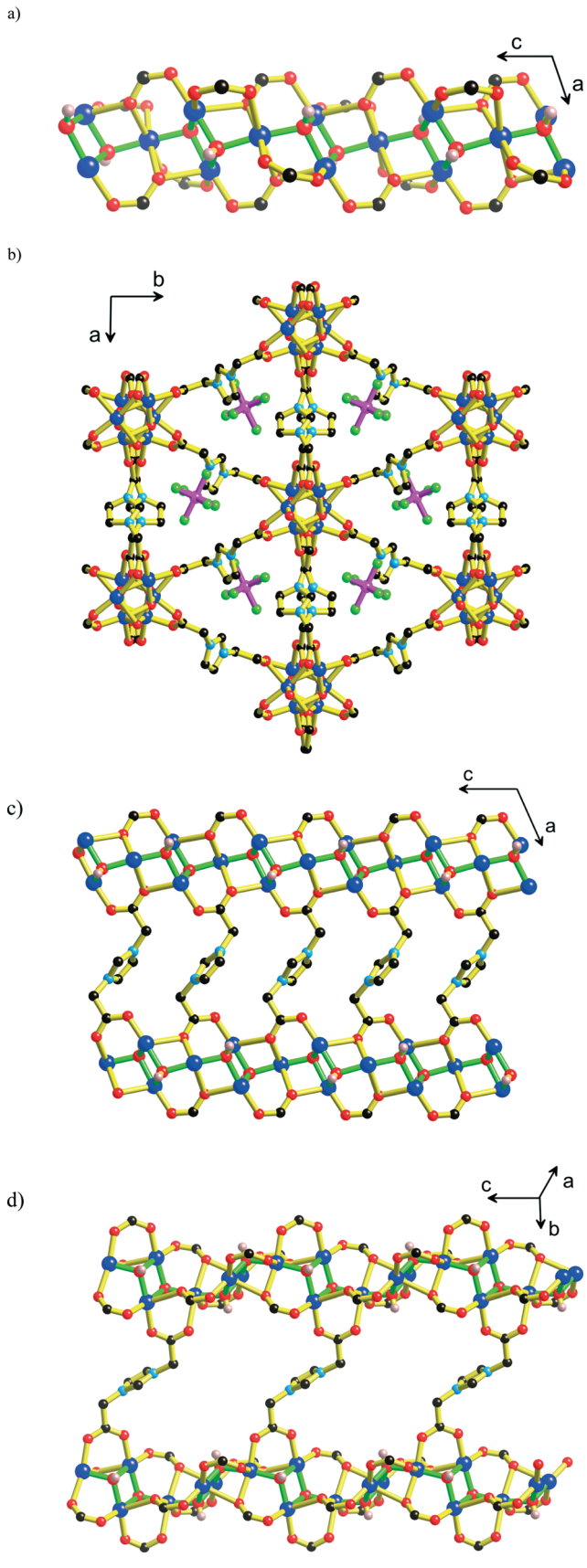

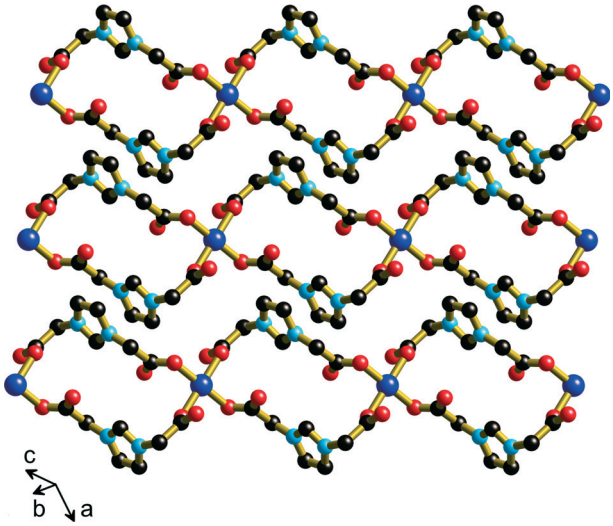

Fig. 5 Three parallel $Cu(imdc)_2$ (**4**) chains; colour code: Cu – deep blue, O – red, N – light blue, C – black.

After further standing, only the second form is present in the reaction mixture.

The blue plate-like crystals of composition $Cu(imdc)_2$, contain chains of the type shown in Fig. 5. All Cu(II) centres are equivalent with a square planar environment provided by carboxylate oxygen donors from four $imdc^-$ ligands, which themselves bridge between two metal centres. Pairs of Cu(II) centres are bridged by two centrosymmetrically related $imdc^-$ ligands, which make moderately close contact with each other (the closest atom-to-atom contact is 3.42 Å, which involves the uncoordinated carboxylate oxygen atom of one $imdc^-$ ligand and the imidazole carbon atom in the 2-position of the other). These chains are able to dovetail snugly together to form sheets, which then stack to afford a relatively dense solid. If the $NaBF_4$ is excluded from the reaction mixture, then the solid product consists solely of $Cu(imdc)_2$ crystals.

The $Cu_2imdc_4NaBF_4{\cdot}7H_2O$ crystals consist of $Cu(imdc)_2$ sheets with the (4,4) topology that exhibit an unusual mode of "perpendicular interpenetration" described below.[7] All sheets, an example of which is shown in Fig 6a, are equivalent. All Cu centres within a sheet are coplanar and are located at the corners of rhombuses (Cu···Cu edge, 9.57 Å; Cu···Cu···Cu angles 99.34 and 80.66°) as can be seen in Fig. 6a. Cu centres are of two types (discussed below), both having an essentially square planar coordination environment of oxygen donors from four $imdc^-$ ligands. All $imdc^-$ units are equivalent and

Fig. 4 The structure of $[Cu_3(OH)_2(imdc)_2]SiF_6$·solvate (**3**) showing a) $Cu_3(OH)_2$ chains (green connections) with carboxylate groups completing the coordination environments of the Cu(II) centres b) the 3D structure viewed down the *c*-direction, SiF_6 anions are indicated by pink bonds c) a channel wall lying parallel with the *a*–*c* plane showing imdc anions linking the $Cu_3(OH)_2$ chains (not all carboxylate groups included) d) one of the channel walls, inclined to the *a*–*c* plane, showing imdc anions linking the $Cu_3(OH)_2$ chains. Colour code: Cu – deep blue, Si – pink, F – green, O – red, N – light blue, C – black; in (a), (c) and (d) hydroxide coordinate bonds are indicated by green connections and only hydroxide hydrogen atoms are indicated.

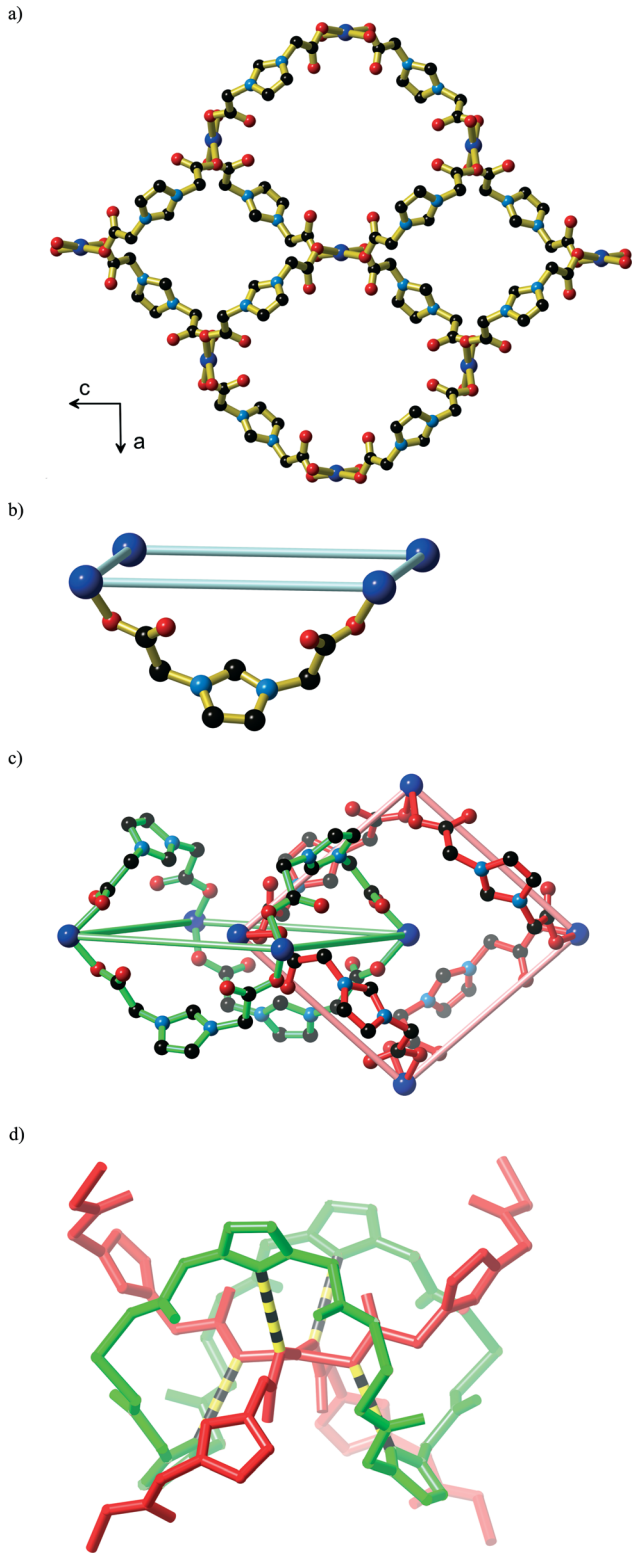

Fig. 6 The structure of $Cu_2imdc_4NaBF_4{\cdot}7H_2O$ (**5**) showing a) part of the 2D $Cu(imdc)_2$ network with the two types of rhombic holes b) four Cu(II) centres which are linked by $imdc^-$ ligands, that loop either above or below the plane of the Cu(II) centres; only one of the four imdc ligands is indicated c) two catenating rings, one from one sheet (red connections) the other from the perpendicular sheet (green connections) d) part of one framework (red connections) passing through one of the congested rings of a perpendicular framework (green connections); C–H···O hydrogen bonds extending from the imidazolium groups of the green framework to coordinated oxygen atoms of the red framework are indicated by yellow and black striped connections.

provide bridges between two metal centres, connecting Cu to Cu along the edges of the Cu_4 rhombuses. The bridges loop well above and below the Cu plane, as shown in Fig. 6b; the van der Waals "thickness" of the resulting network corresponds to the length of the *a* axis (12.3883(3) Å). Although the Cu···Cu separations across the Cu(imdc)Cu linkages are all the same (9.57 Å), there are nevertheless, as inspection of Fig. 6a will reveal, two types of hole at the centres of the rhombuses, one visibly more congested than the other. This distinction arises from different geometries of attachment of $imdc^-$ ligands to metal (whether *cis* or *trans*); the bridging $imdc^-$ ligands along the edges of the more open hole are connected to the Cu centres at the corners in a *trans* relationship, as can be seen in Fig. 6a, whereas the bridging ligands along the edges of the more congested holes are attached to the Cu corners in a *cis* fashion. The four bridging ligands that form the perimeter of the congested hole adopt conformations in which the C–H bond involving the carbon at the 2-position of the imidazole ring is directed towards the centre of the hole. There are two different types of Cu centre: Cu1 is found on the long diagonals of the less congested Cu_4 rhombuses and Cu2 on the long diagonals of the more congested rhombuses.

Parallel sheets related by a pure translation stack directly on top of each other. Every sheet is intersected by an infinite number of perpendicular ones in the manner shown schematically in Fig. 7a, in which individual sheets are represented as Cu centres connected together by imaginary rods. A line of intersection can be envisaged where two perpendicular sheets interpenetrate and, as can be seen in Fig. 7a, it is along this line that Cu centres from both 2D nets can be found; Cu centres of either sheet can be seen located at the centres of the Cu_4 rhombuses of the other sheet. The intersection occurs specifically along the long diagonals of the more congested rhombuses and it is specifically Cu2 centres from both sheets that are located along this line. The essence of the interpenetration, the feature repeated over and over again throughout the entangled structure, is shown in Fig. 6c, which represents two of the more congested rings, one from one sheet the other from the perpendicular sheet, catenated together with their long diagonals aligned along the line of intersection. Close inspection of the interaction between the two networks reveals a quartet of complementary C–H···O hydrogen bonds involving C atoms in the 2-position of the imidazolium ring and the coordinated oxygen atoms bound to Cu2 (Fig. 6d).

An interesting feature of the structure is the incorporation of hydrated Na^+ and BF_4^- ions in the structure. The Na^+ ions are disordered over four closely separated sites and are bound to six water molecules. These hydrated cations are located within the less congested holes of the $Cu(imdc)_2$ networks. The BF_4^- anions are disordered over two closely separated sites (see ESI† for further details relating to the disorder in the structure). As noted above, when the reaction is repeated in the absence of $NaBF_4$ then the 1D polymer, $Cu(imdc)_2$, is the sole product. It therefore seems likely that

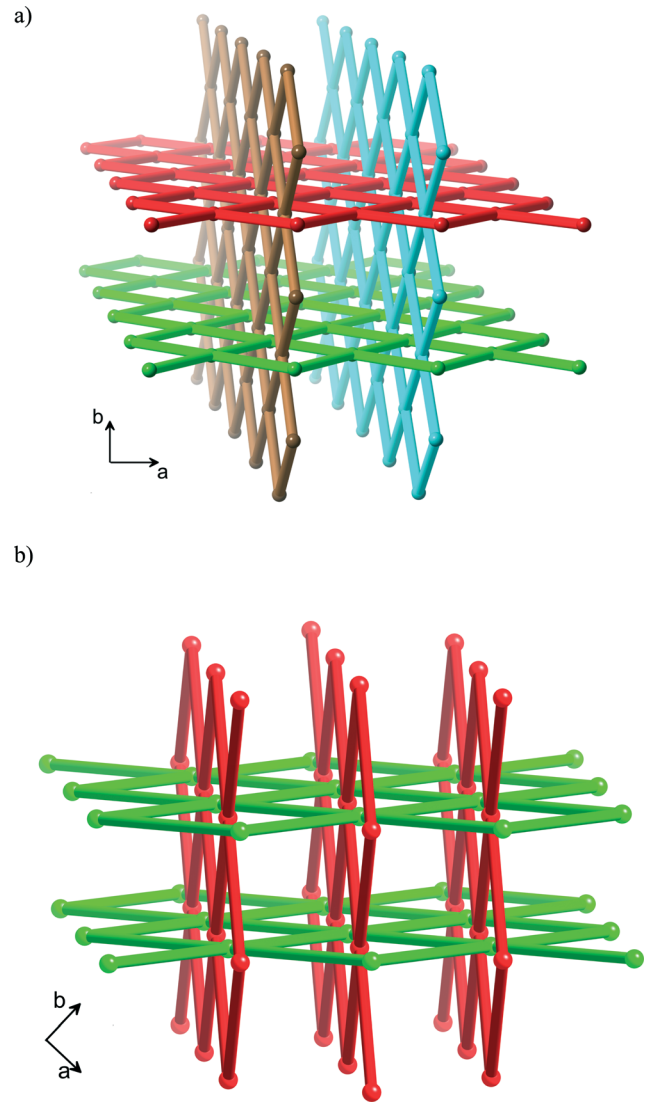

Fig. 7 Schematic representations of the interpenetration of "square-grid" sheets in a) $Cu_2imdc_4NaBF_4{\cdot}7H_2O$ (**5**); b) $Zn(4,4'bipy)_2SiF_6{\cdot}2H_2O$.[8] Spheres represent metal centres whilst the bridging ligands are represented by the connections.

the hydrated Na^+ and BF_4^- ions play a templating role in the assembly of the interpenetrating structure. Infinite chains of alternating hydrated Na^+ and BF_4^- ions extend in directions parallel to both the *a* and *b* axes.

The type of interpenetration shown in Fig. 7a is related to an archetypal mode of sheet/sheet interpenetration first seen in $Zn(4,4'\text{-bipyridine})_2(SiF_6)$[7,8] and shown in Fig. 7b. The mode of interpenetration seen in $Cu_2imdc_4NaBF_4{\cdot}7H_2O$ differs from the archetypal "perpendicular interpenetration" in that only half the available holes are involved in the intermeshing – the less congested holes do not have elements of other sheets passing through them.

The structure provides an interesting contrast with a topologically similar but neutral network of composition $Cd(imdc)_2$ in which 8-coordinate Cd(II) centres are bridged by four $imdc^-$ ligands within a square grid sheet.[3c] In the Cd structure the sheets are arranged in a manner that does not leave spaces between the sheets, furthermore the sheets stack in an A, B, A, B… manner that does not allow channel formation along the stacking direction.

General comments

The variability in the composition of the compounds within the series of structures provides an opportunity to examine how the coordination environment of Cu(II) changes in response to the number of available carboxylate groups. Whilst the two $Cu(imdc)_2$ polymeric structures have different dimensionalities (1D for **4** and 2D for **5**) both structures, which have a carboxylate to metal ratio of 4 : 1, include square planar Cu(II) centres formed by the oxygen atoms of four monodentate carboxylate groups. When the carboxylate to Cu(II) ratio is 2 : 1, as it is in the solvated and desolvated forms of $Cu_2(imdc)_2(BF_4)_2$ (**1** and **2** respectively) the carboxylate anions are now bidentate and the carboxylate groups bridge a pair of Cu(II) centres as it does in the copper(II) acetate dimer. With the discrete binuclear Cu(II) unit serving as a 4-connecting node a 2D network is generated. In the structure of $[Cu_3(OH)_2(imdc)_2]{\cdot}SiF_6{\cdot}2H_2O{\cdot}2MeOH$ the ratio of carboxylate to Cu(II) is reduced even further to 4 : 3 following incorporation of hydroxide into the network. In this structure infinite chains of closely separated Cu(II) centres, linked by hydroxide anions, are bridged by μ_2 and μ_3 carboxylate groups resulting in a 3D network. The structures presented in this current work provide an illustration of the variability in the coordinating behaviour of carboxylate groups with Cu(II) and an indication of the impact such coordination modes have on the connectivity of the resulting coordination polymers.

Conclusion

To the best of our knowledge this is the first report of crystal structures involving copper complexes of the "zwitterion", $imdc^-$, a ligand that incorporates two anionic carboxylate groups but overall, possesses only a single negative charge. Whilst factors such as the coordination mode of a ligand and a metal centre's preference for certain coordination geometries play an expected major role in governing the topology and geometry of a coordination network, more subtle factors such as the presence of guest species can also have a significant influence on the resulting structure. This is very clearly evident in the two "$Cu(imdc)_2$" structures where the incorporation of solvated Na^+ and BF_4^- ions gives rise to unusual interpenetrated 2D sheets in contrast to the chain structure containing only Cu^{2+} and $imdc^-$ ions in a 1 : 2 ratio. Although the contrast is not as stark between the solvated and desolvated forms of $Cu_2(imdc)_2(BF_4)_2$ significant structural changes are apparent in a remarkable transformation that occurs with retention of single crystal character.

Experimental

$H_2imdc{\cdot}Cl$ was prepared from the reaction of imidazole and methyl chloroacetate. Subsequent hydrolysis of the diester

with dilute acid, as per the synthetic procedures established by Dyson *et al.*,[9] was performed. Following a similar process outlined by Dyson *et al.*[10] Himdc was prepared by stirring a mixture of H_2imdc·Cl and triethylamine in dichloromethane overnight. Solid Himdc was removed by filtration and recrystallized from hot water.

Synthesis of $[Cu_2(imdc)_2(CH_3OH)_2](BF_4)_2$·solvate

H_2imdc·Cl (45 mg, 0.20 mmol) was added to a solution containing $Cu(BF_4)_2$ in water (1 mL, 0.25 mol L^{-1}) and CH_3OH (12 mL). The capped reaction mixture was allowed to stand. After 48 hours blue block-like crystals separated from the solution, yield 29 mg. Elemental analysis was performed on a sample that had been filtered and dried in the atmosphere. Analysis calculated for $[Cu_2(imdc)_2(CH_3OH)(H_2O)](BF_4)_2·2H_2O$: C 23.9, N 7.4, H 3.2%. Found C 24.0, N 7.4, H 3.5%.

Synthesis of $[Cu_2(imdc)_2(BF_4)_2]$

Crystals of [Cu(imdc)(MeOH)]·BF_4·solvate were heated at 135 °C in an oven for 1 hour. The heated crystals were transferred directly from the oven into protective oil before placed on the diffractometer in a stream of nitrogen at 130 K.

$[Cu_3(OH)_2(imdc)_2]SiF_6$·solvate

A 4 mL aqueous solution containing, Himdc (45 mg, 0.24 mmol), $Cu(OAc)_2·H_2O$ (106 mg, 0.53 mmol) and $CuSiF_6$ (48 mg, 0.23 mmol) was mixed with 3 mL of MeOH and the reaction mixture was sealed. Light blue crystals formed over a period of 24 hours. The crystals were collected, washed with acetone and dried in air, yield 40 mg. Analysis calculated for $[Cu_3(imdc)_2(OH)_2]SiF_6·4.5H_2O$: C 20.50, H 3.22, N 7.16. Found C 20.67, H 3.04, 6.73%.

$[Cu(imdc)_2]$

Himdc (50 mg, 0.27 mmol) and $Cu(OAc)_2·H_2O$ (55 mg, 0.28 mmol) were dissolved in 1 mL of water. 5 mL of methanol was added to this solution, which was then sealed. Blue plate-like crystals formed over a period of 24 hours. The crystals were collected, washed with acetone and dried over air. Yield: 18 mg. Analysis calculated for $Cu(imdc)_2·H_2O$: C 37.54, H 3.61, N 12.51%. Found C 37.86, H 3.47, N 12.43%.

$Cu_2(imdc)_4NaBF_4·7H_2O$

Himdc (50 mg, 0.27 mmol), $Cu(OAc)_2·H_2O$ (55 mg, 0.28 mmol) and $NaBF_4$ (30 mg 0.27 mmol) were dissolved in 2 mL of water. 5 mL of methanol was added to this solution, which was then sealed. Over a period of 24 hours a combination of blue octahedral crystals and blue plate crystals separated from the reaction mixture. X-ray analysis indicated the blue octahedral crystals were composed of 2-D interpenetrating sheets, whilst the plate-like crystals were shown to be $[Cu(imdc)_2]$ (described above). The infrared spectrum (ESI,† Fig. S2b) of manually separated crystals of $Cu_2(imdc)_4NaBF_4·7H_2O$ indicated the presence of BF_4^- ions. Over a period of 48 hours the octahedral crystals redissolved in the methanolic mother-liquor and more plate-like crystals separated from the solution.

Single crystal X-ray diffraction studies

Data were collected on an Oxford Diffraction Supernova diffractometer using CuKα radiation. In general crystals were transferred directly from the mother liquor to a protective oil before being mounted on the diffractometer in a stream of nitrogen at 130 K. In the case of compound 2 crystals of compound 1 were dried in an oven and transferred directly to a

Table 1 Crystal structure and refinement details

Compound	1	2	3	4	5
Formula	$C_{17}H_{28}N_4O_{12}B_2F_8Cu_2$	$C_{14}H_{14}N_4O_8B_2F_8Cu_2$	$C_{16}H_{28}N_4O_{14}SiF_6Cu_3$	$C_{14}H_{14}N_4O_8Cu$	$C_{28}H_{42}N_8O_{23}BF_4NaCu_2$
M	781.13	666.99	833.13	429.83	1095.58
T, K	130(2)	130(2)	130(2)	130(2)	130(2)
Crystal system	Orthorhombic	Orthorhombic	Monoclinic	Triclinic	Tetragonal
Space group	*Pnma*	*Pnma*	*Cc*	$P\bar{1}$	$P\bar{4}2c$
a, Å	16.6263(3)	15.6203(16)	12.4176(2)	7.1674(6)	12.3883(3)
b, Å	12.7971(3)	11.564(2)	22.5346(3)	7.5711(8)	12.3883(3)
c, Å	14.4678(3)	14.8705(14)	10.1644(2)	8.4825(11)	14.5923(4)
α, °	90	90	90	109.937(11)	90
β, °	90	90	107.054(2)	94.919(8)	90
γ, °	90	90	90	116.156(9)	90
V, Å^3	3078.29(11)	2686.1(6)	2719.19(8)	372.90(7)	2239.48(10)
Z	4	4	4	1	2
μ, mm^{-1}	2.715	2.889	4.233	1.914	2.236
Measured reflns	7668	9024	9363	2302	4291
Unique reflns	3145	2568	3687	1447	1805
R_{int}	0.0186	0.1062	0.0256	0.0209	0.0196
Obs reflns [$I > 2\sigma(I)$]	2818	1340	3562	1395	1647
Parameters	237	204	420	124	155
Flack parameter			0.01(3)		0.01(8)
GOF on F^2	1.163	0.970	1.056	1.331	1.073
$R_1[I > 2\sigma(I)]$	0.0578	0.0784	0.0266	0.0836	0.0569
wR_2 (all data)	0.1597	0.2428	0.0699	0.3181	0.1715

protective oil before being mounted on the diffractometer in a stream of nitrogen at 130 K. Structures were solved by direct methods and refined using a full matrix least-squares procedure based on F^2 (SHELX97).[11] The crystallographic analyses were performed using the WinGX system of programs.[12] Crystal data and refinement details are presented in Table 1.

Powder diffraction

Powder-XRD data for the compounds $[Cu_2(imdc)_2(CH_3OH)_2]\cdot 2BF_4(CH_3OH)(H_2O)$ (**1**) $Cu(imdc)_2$ (**4**) and $Cu_2(imdc)_2\cdot NaBF_4\cdot 7H_2O$ (**5**) were collected at the powder diffraction beamline at the Australian Synchrotron using radiation with λ = 0.7907 Å. The data were measured at 300 K. The powder diffraction pattern for $[Cu_2(imdc)_2(BF_4)_2]$ (**2**) and $[Cu_3(OH)_2(imdc)_2]SiF_6\cdot 2H_2O\cdot 2MeOH$ (**3**) were collected on an Oxford SuperNova diffractometer using CuKα radiation λ = 1.5418 Å. The measurements were performed at 293 K. For compounds **1–5** the powder diffraction data of the bulk product matched the simulated diffraction data obtained from the single crystal structure determination.

Gas sorption

Crystals of **1** were transferred from the mother liquor into a sample cell and dried under dynamic vacuum at 120 °C. CO_2 isotherms were measured at 258 and 273 K using a Sieverts-type BEL-HP automatic high pressure gas sorption instrument (BEL Japan Inc.). The temperature of the sample was controlled using a Julabo F25-ME chiller/heater. The heat of CO_2 sorption was calculated using a virial-type thermal adsorption equation which models ln(P) as a function of the volume of surface excess gas sorbed by the solid over all measurement temperatures.[13]

Thermogravimetic data

Thermogravimetric analysis measurements were performed using an SDTA851 analyser. Isothermal and dynamic measurements from room temperature to 450 °C were carried out on solid samples of compounds under an N_2 atmosphere. 40 μL aluminium crucibles were used.

Infrared spectra

Infrared spectra were collected on a Bruker Tensor 27 FTIR.

Elemental analysis

Microanalyses were performed at, Campbell Microanalytical Laboratory Dunedin, New Zealand.

Acknowledgements

We gratefully acknowledge the financial support provided by the Australian Research Council. This research is supported by the Science and Industry Endowment Fund. Part of the work reported was undertaken on the powder diffraction beamline at the Australian Synchrotron, Victoria, Australia.

References

1 (*a*) Z. Fei, T. J. Geldbach, R. Scopelliti and P. J. Dyson, *Inorg. Chem.*, 2006, **45**, 6331; (*b*) Z. Fei, T. J. Geldbach, D. Zhao, R. Scopelliti and P. J. Dyson, *Inorg. Chem.*, 2005, **44**, 5200.

2 (*a*) X.-W. Wang, L. Han, T.-J. Cai, Y.-Q. Zheng, J.-Z. Chen and Q. Deng, *Cryst. Growth Des.*, 2007, **7**, 1027; (*b*) X.-C. Chai, H.-H. Zhang, S. Zhang, R. Lei, Y.-P. Chen, Y.-Q. Sun, R.-Q. Sun and Q.-Y. Yang, *Chin. J. Struct. Chem.*, 2009, **28**, 1343.

3 (*a*) Z. Fei, W.-H. Ang, T. J. Geldbach, R. Scopelliti and P. J. Dyson, *Chem.–Eur. J.*, 2006, **12**, 4014; (*b*) Z. Fei, D. Zhao, T. J. Geldbach, R. Scopelliti, P. J. Dyson, S. Antonijevic and G. Bodenhausen, *Angew. Chem., Int. Ed.*, 2005, **44**, 5720; (*c*) X.-F. Zhang, S. Gao, L.-H. Huo and S. W. Ng, *Acta Crystallogr., Sect. E: Struct. Rep. Online*, 2006, **62**, m2910; (*d*) X.-F. Zhang, S. Gao, L.-H. Huo and S. W. Ng, *Acta Crystallogr., Sect. E: Struct. Rep. Online*, 2006, **62**, m3359; (*e*) X.-F. Zhang, S. Gao, L.-H. Huo and S. W. Ng, *Acta Crystallogr., Sect. E: Struct. Rep. Online*, 2006, **62**, m3365; (*f*) X.-F. Zhang, S. Gao, L.-H. Huo and S. W. Ng, *Acta Crystallogr., Sect. E: Struct. Rep. Online*, 2006, **62**, m3418.

4 (*a*) L. Han, S. Zhang, Y. Wang, X. Yan and X. Lu, *Inorg. Chem.*, 2009, **48**, 786; (*b*) X.-C. Chai, Y.-Q. Sun, R. Lei, Y.-P. Chen, S. Zhang, Y.-N. Cao and H.-H. Zhang, *Cryst. Growth Des.*, 2010, **10**, 658.

5 S. Brunauer, L. S. Deming, W. E. Deming and E. Teller, *J. Am. Chem. Soc.*, 1940, **62**(7), 1723.

6 (*a*) H.-S. Choi and M. P. Suh, *Angew. Chem., Int. Ed.*, 2009, **48**, 6865; (*b*) H. J. Park and M. P. Suh, *Chem. Commun.*, 2010, **46**, 610; (*c*) J. Seo, R. Matsuda, H. Sakamoto, C. Bonneau and S. Kitagawa, *J. Am. Chem. Soc.*, 2009, **131**, 12792; (*d*) K. Tanaka, K. Nakagawa, M. Higuchi, S. Horike, Y. Kubota, T. Kobayashi, M. Takata and S. Kitagawa, *Angew. Chem., Int. Ed.*, 2008, **47**, 3914; (*e*) Y. Inubushi, S. Horike, T. Fukushima, G. Akiyama, R. Matsuda and S. Kitagawa, *Chem. Commun.*, 2010, **46**, 9229; (*f*) B. F. Abrahams, M. J. Grannas, L. J. McCormick, R. Robson and P. J. Thistlethwaite, *CrystEngComm*, 2010, **12**, 2885.

7 S. R. Batten and R. Robson, *Angew. Chem., Int. Ed.*, 1998, **37**, 1460.

8 R. W. Gable, B. F. Hoskins and R. Robson, *J. Chem. Soc., Chem. Commun.*, 1990, 1677.

9 Z. Fei, D. Zhao, T. J. Geldbach, R. Scopelliti and P. J. Dyson, *Chem.–Eur. J.*, 2004, **10**, 4886.

10 A. D. Phillips, Z. Fei, W. H. Ang, R. Scopelliti and P. J. Dyson, *Cryst. Growth Des.*, 2009, **9**, 1966.

11 G. M. Sheldrick, *Acta Crystallogr., Sect. A: Found. Crystallogr.*, 2008, **64**, 112.

12 L. J. Farrugia, *J. Appl. Crystallogr.*, 1999, **32**, 837.

13 L. Czepirski and J. Jagiello, *Chem. Eng. Sci.*, 1989, **44**, 797.